Proceedings of the 1st Marine Energy Technology Symposium
METS13
April 10-11, 2013, Washington, D.C.

IMPLICATIONS OF TIDAL PHASING FOR POWER GENERATION AT A TIDAL ENERGY SITE

Brian Polagye[1]
University of Washington,
NNMREC
Seattle, WA, USA

Jim Thomson
University of Washington,
NNMREC
Seattle, WA, USA

[1]Corresponding author: bpolagye@uw.edu

ABSTRACT

Spatial resource gradients have been observed at a number of proposed tidal energy sites. However, these gradients are typically quantified using the first or second moments (i.e., mean or standard deviation) of time series which obscures information about the co-temporal amplitude and phase variation. These co-temporal variations have a number of interesting implications for power production from arrays of tidal turbines. Here, co-temporal time series data from several locations in northern Admiralty Inlet, Puget Sound, Washington (USA) are used to investigate phase variations in kinetic power density over length scales of less than 5 km. Results demonstrate that large phase variations in kinetic power density are routinely produced by phase variations in the harmonic and aharmonic currents. However, exploiting these phase variations in a way that reduces power generation intermittency requires that locations which are out of phase have similar mean kinetic power density and intermittency. Further investigation of local phasing at tidal energy sites of commercial interest is recommended.

INTRODUCTION

Resource characterization is an essential early-stage activity in tidal energy project development. The information obtained feeds into structural load calculations, as well as estimates for power generation from individual turbines or small arrays. [1] present a set of resource metrics that describe characteristics of the mean (as opposed to turbulent) currents at potential turbine deployment locations within Admiralty Inlet, Puget Sound, WA (USA). These are statistical quantities either averages (first moment) or variances (second moment), which obscure information about co-temporal amplitude and phase variations between locations. These variations can have a number of interesting implications for power production from arrays. For example, if the amplitude of the currents is similar at two locations, but the currents are out of phase, their aggregate power generation profile will be more continuous than for the individual locations. The potential to benefit from "tidal phasing" has been investigated at a national scale by Iyer et al. [2], but has not been investigated at smaller scales. Here, we investigate tidal phasing within a single site over length scales less than 5 km.

METHODOLOGY

Site Description

Admiralty Inlet is the primary entrance to Puget Sound, branching southeast from the junction of the Strait of Juan de Fuca and Strait of Georgia. Excepting a small tidal exchange through Deception Pass to the north, the entirety of Puget Sound's tidal prism passes through Admiralty Inlet. The northern inlet is relatively shallow (80 m deep) and narrow (5 km wide) in comparison to the adjacent waters and this geographic constriction gives rise to tidal currents exceeding 3 m/s [3].

The strength of these currents has motivated interest in developing a tidal current energy project in northern Admiralty Inlet. Public Utility No. 1 of Snohomish County has proposed a multi-year demonstration project (e.g., installed capacity of less than 1 MW) at this location to develop environmental and engineering data needed to assess the feasibility of a commercial-scale project (e.g., installed capacity greater than 10 MW).

Data Collection

Since 2009, instrumentation has been deployed in northern Admiralty Inlet to characterize the biological and physical

TABLE 1. DOPPLER PROFILER DEPLOYMENT DETAILS.

Deployment Pair	Location	Site Type	Separation	Comparison Dates	Profiler Type	Bin Size	Range	Ensemble Interval
I	A	Near-headland	56 m	5/11 – 8/9/2011	1	1 m	41 m	60 s
	B	Near-headland			2	1 m	40 m	60 s
II	A	Near-headland	67 m	7/5 – 8/9/2011	1	1 m	41 m	60 s
	C	Near-headland			3	1 m	25 m	1 s
III	D	Near-headland	81 m	8/17 – 9/19/2011	1	1 m	45 m	60 s
	E	Eddy apex			3	1 m	20 m	60 s
IV	A	Near-headland	2600 m	2/13 – 5/9/2011	1	1 m	50 m	60 s
	F	Center channel			2	1 m	40 m	1 s

Profiler Types – 1: 470 kHz Nortek Continental; 2: 600 kHz Nortek AWAC; 3: 1000 kHz Nortek AWAC

environment in support of tidal energy development. These bottom packages, assembled around Sea Spider frames (Oceanscience, Ltd.) are instrumented with acoustic Doppler current profilers, broadband hydrophones, cetacean click detectors, fish tag receivers, and water quality sensors. The locations and details of Doppler profiler deployments analyzed in this study are presented in Figure 1 and Table 1, respectively. Four pairs of co-temporal profiler deployments are considered. The first two pairs (I and II) are separated by less than 70 m and located approximately 1 km southwest of Admiralty Head (land mass on right margin of bottom panel of Figure 1). The third pair (III) is separated by a similar distance, but located slightly closer to the headland. Site E, in particular, is located at the intersection of the gravel waves that demarcate the extent of the eddies that form to either side of the headland on ebb and flood. Consequently, this is likely to be the most energetic site near the headland and have the most pronounced spatial variations in resource intensity. The final pair (IV) is separated by 2600 m and allows a comparison of mid-channel and near-headland locations.

Kinetic Power Density

For each five-minute speed ensemble, the kinetic power density (K) was calculated as

$$K(t) = 1/2\,\rho U(t)^3 \qquad (1)$$

where ρ is the density of seawater (1025 kg/m^3) and U is the 5-minute average horizontal current speed centered at time t. The time-averaged kinetic power density over each deployment was then calculated to produce a temporally unresolved comparison metric for pairs of sites.

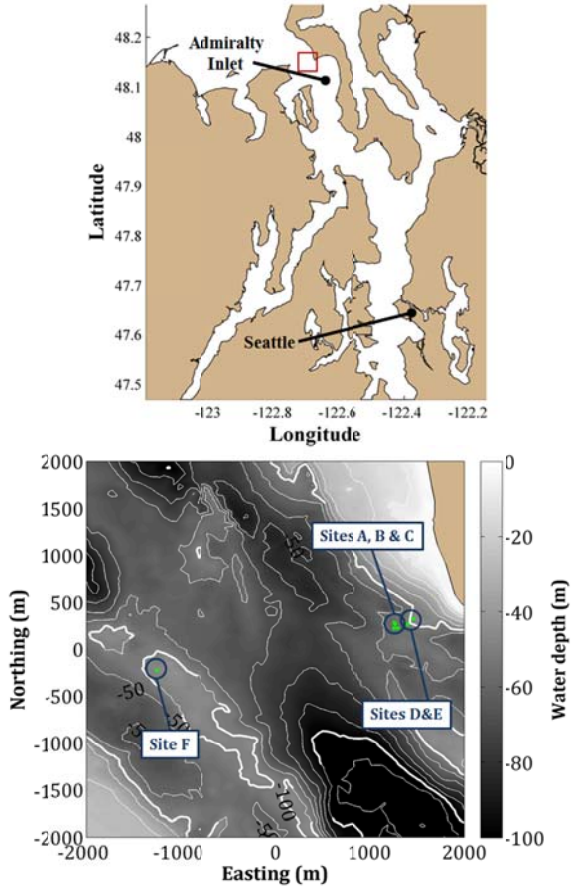

FIGURE 1. (TOP) ADMIRALTY INLET GEOGRAPHY AND (BOTTOM) DOPPLER PROFILER DEPLOYMENT LOCATIONS WITHIN AREA OF DETAIL IDENTIFIED ON REGIONAL MAP.

To quantify co-temporal amplitude and phase variations for deployment pairs, the time-varying kinetic power density difference (ΔK) between

each station in a deployment pair was calculated as

$$\Delta K(t) = K_2(t) - K_1(t) \quad (2)$$

for each point in the series (where 1 and 2 denote the first and second sites for the deployment pairs listed in Table 1). For a given K_1, the probability of ΔK taking on a particular value was calculated (i.e., given that K_1 was X kW/m^2, what was the probability of K_2 being higher or lower by ΔK kW/m^2?).

Harmonic Current Phase

The time-variation in tidal elevation (h) may be compactly represented as the superposition of multiple "constituents" with globally-defined periods and locally varying amplitude and phase as

$$h(t) = \sum A_i \sin\left(\frac{2\pi t}{T_i} + g_i\right) \quad (3)$$

where A_i, g_i, and T_i are the amplitude, phase, and period of the i^{th} tidal constituent [5]. Each constituent represents a periodicity in the relative position or orientation of the earth, moon, and sun. The harmonic component of the tidal currents may be similarly approximated, but the aharmonic response (i.e., changes to the flow induced by local topography or bathymetry, such as large-scale eddies shed by headlands [e.g., **6**]), density-driven circulation, storm surges, waves, and turbulence may also contribute to observed currents at tidal energy sites [**1**]. The averaging period used here (5 minutes) removed most of the turbulent energy from observations, and at this depth neither wave orbital velocity nor density-driven circulation was significant. Consequently, harmonic analysis was be employed to investigate the extent to which variations in the phase of the tidal between locations was attributable to the harmonic component of the tide, as opposed to the aharmonic component. The amplitudes phases of the dominant semidiurnal (M2) and diurnal (K1) tidal current constituents were obtained for each site pair using the package U_TIDE [**7**]. U_TIDE is a recent enhancement to T_TIDE [8]. For this analysis, the Ordinary Least Squares (OLS) solver was employed, the signal to noise ratio for constituent inclusion was set to 3, and the Rayleigh criteria was set to 1. As discussed in the results, harmonic analysis for each pair of sites was performed only on the co-temporal portions of the measurement time series.

Implications of Phasing for Power Intermittency

The practical implications of co-temporal amplitude and phase variations in kinetic power density were evaluated in a two-step procedure. First, $K(t)$ at a given site was converted to a turbine-adjusted value (P) that accounted for the non-linear effect of rated and cut-in speeds as

$$P(t) = \begin{cases} 0 & U(t) < U_{\text{cut-in}} \\ K(t) & U_{\text{cut-in}} \geq U(t) \leq U_{\text{rated}} \\ 1/2\,\rho U_{\text{rated}}^3 & U(t) > U_{\text{rated}} \end{cases} \quad (4)$$

where $U_{\text{cut-in}}$ is the turbine cut-in speed and U_{rated} is the turbine rated speed. $U_{\text{cut-in}}$ was set to 0.7 m/s, in line with expectations for utility-scale turbines, and U_{rated} was selected to achieve a capacity factor of approximately 30% (for the specific case considered, 2.0 m/s). The capacity factor (CF) for an array of turbines at a specific location was defined as

$$CF = \langle P \rangle / P_{\text{rated}} \,. \quad (5)$$

The standard deviation of the P was also calculated (i.e., σ_P) as measure of the intermittency of power output from a turbine deployed at a specific location. This is of interest because reduced intermittency should increase the value of the power provided by an array of tidal current turbines. To evaluate the potential for phasing to reduce intermittency, scenarios were constructed that involved arrays at a pair of locations with different kinetic power amplitudes and phases, but identical combined mean power (turbine-adjusted). The standard deviations of the turbine-adjusted power density for the hybrid arrays were calculated and compared to a reference value for an array at a single location. Implicit in this calculation was assumption that the co-temporal phase variations in power density would not be changed by extracting power. This is a site-specific consideration that is likely best addressed by numerical simulation. However, for arrays which extract a small fraction of the natural power dissipated in a region, the assumption is likely valid.

RESULTS

Kinetic Power Density

Table 2 shows the mean (time-averaged) kinetic power density for each location, averaged over the deployment duration, as well as the mean water depth. For deployment pairs I and II, the mean power densities at sites B and C are ~10% higher than at site A. For pair III, the difference in

mean power density is more pronounced, with site E ~20% more energetic than site D (even though the separation distance is similar to the separation between sites A, B, and C). For pair IV, the center channel (site F) is ~20% less energetic than the headland (site A). While the mean power density for site A is calculated over two different ~90 day periods for pairs I/II and pair IV, there are only small variations in this quantity for reasons described in [1].

Figure 2 through Figure 5 show representative time series of power density and statistical information about power density phasing for deployment pairs I-IV. In all four figures, the conditional probability of power density (bottom panels) saturate at 15%. Visual examination of the co-temporal time series (Figure 2, top panel) demonstrates that sites A and B are in phase, with site B, on average, ~10% more energetic than site A. Pair II (Figure 3) is quite similar, with the two sites in phase, but with moderate differences in mean power density. As shown in Figure 4, currents at sites D and E are sometimes in phase (top panel) with currents at site E generally more intense (left branch of probability density in bottom panel). However, at some stages of the tide there is a non-zero probability of site D being more energetic than site E (right branch of probability density in bottom panel).

For pair IV, the phase differences between the headland (site A) and center channel (site F) are more complex. During the greater tides of the diurnal inequality (Admiralty Inlet is a mixed, mainly semi-diurnal tidal regime with four tidal exchanges each day, but of unequal strength), the two sites are in phase over the majority of the tidal cycle (first twelve hours of Figure 5, top panel). During the second exchange, even though site A is ~20% more energetic, on average, than site F, the power density at site F can be temporarily greater than at site A. Specifically, at the end of second greater tide, the power density at site F is twice that of site A. On the third exchange, the two sites are almost entirely out of phase and have unequal resource intensities, but on the fourth, weakest exchange, they are back in phase with nearly equal intensities. This suggests a complicated underlying physical mechanism, possibly related to the dynamics of eddy formation around the headland. This complexity is reflected in the kinetic power phase statistics shown in the bottom panel of Figure 5. It is possible for currents to be nearly quiescent near the headland (i.e., 0 kW/m^2 at site A) while power density is operationally significant (i.e., capable of generating electricity) in the center of the channel. Similarly, even though site F is, on average, less

TABLE 2. MEAN KINETIC POWER DENSITY (20 m ABOVE SEABED).

Pair	Site	<*K*> (kW/m^2)	Mean depth (m)
I	A	1.7	60
	B	1.9	61
II	A	1.7	60
	C	1.9	61
III	D	1.9	54
	E	2.3	58
IV	A	1.6	59
	F	1.3	49

energetic than site A, there are times when power density at site F is almost triple that of site A (e.g., ~10 kW/m^2 difference between sites when the power density at the near-headland site is ~5 kW/m^2 as demonstrated by extreme of the left branch of the probability density).

Harmonic Current Phase

Table 3 shows the amplitude (*A*) and phase (*g*) of the principal semidiurnal (M2) and diurnal (K1) tidal current constituents for each pair of comparison sites, along with the confidence intervals in these estimates, as predicted by U_TIDE. For Site A, these amplitudes and phases are estimated over different date ranges for different comparison pairs (Table 1). While the different estimates for the phase of the M2 constituent fall within the range of uncertainty given by its confidence interval, the M2 amplitude estimates, as well as K1 phase and amplitude estimates fall outside of these bounds. The uncertainties in these constituent amplitudes and phases estimated in Kutney et al. [9] from an annual time series are significantly greater than those estimated by U_TIDE. As discussed in [9], this has implications for calculating Annual Energy Production (AEP) using harmonic predictions. However, for the present purposes of evaluating kinetic power phase differences between locations, the relative bias is likely negligible for constituents that have been estimated from co-temporal time series.

Pairs I and II (sites A/B and B/C) have nearly identical phases for the M2 and K1 constituents, as would be expected from the descriptions of power density phasing in Figure 2 and Figure 3. Pair III (sites D and E) also has nearly identical K1 and M2 phases, though, as demonstrated by Figure 4, the power density is not always in phase between these locations. Pair IV (sites A and F) has a substantial phase difference for the M2 constituent, but nearly identical phase for the K1 constituent. While this difference in constituent phase suggests that the power density between the sites should be out of phase, it does not intuitively explain the trends shown in Figure 5.

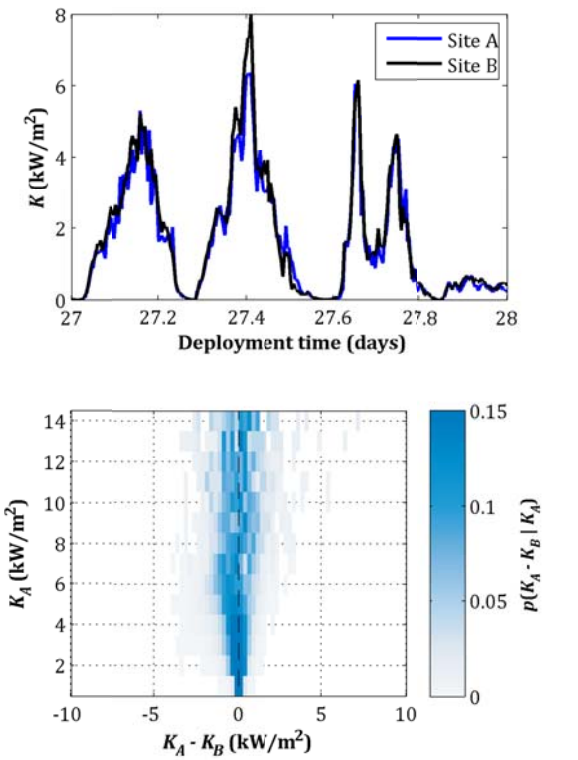

FIGURE 2. (TOP) REPRESENTATIVE TIME SERIES VARIATIONS IN POWER DENSITY BETWEEN SITES A AND B. (BOTTOM) POWER DENSITY PHASE PROBABILITY FOR SAME SITES.

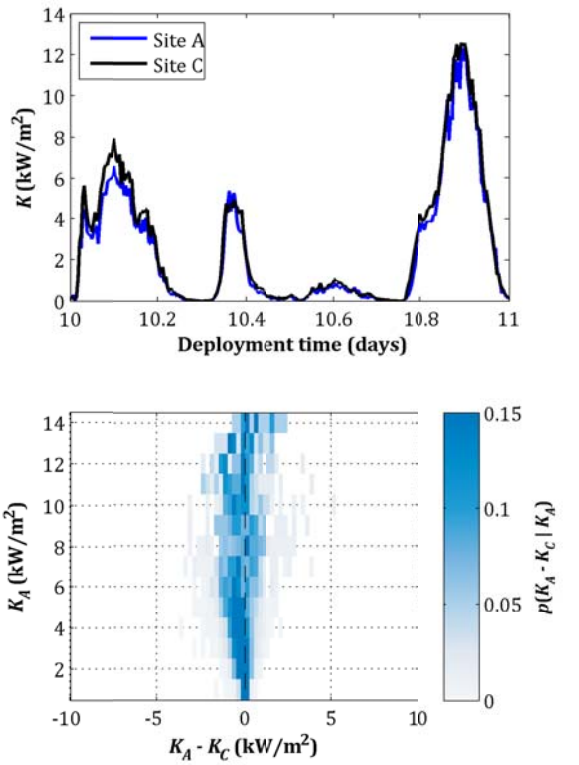

FIGURE 3. (TOP) REPRESENTATIVE TIME SERIES VARIATIONS IN POWER DENSITY BETWEEN SITES A AND B. (BOTTOM) POWER DENSITY PHASE PROBABILITY FOR SAME SITES.

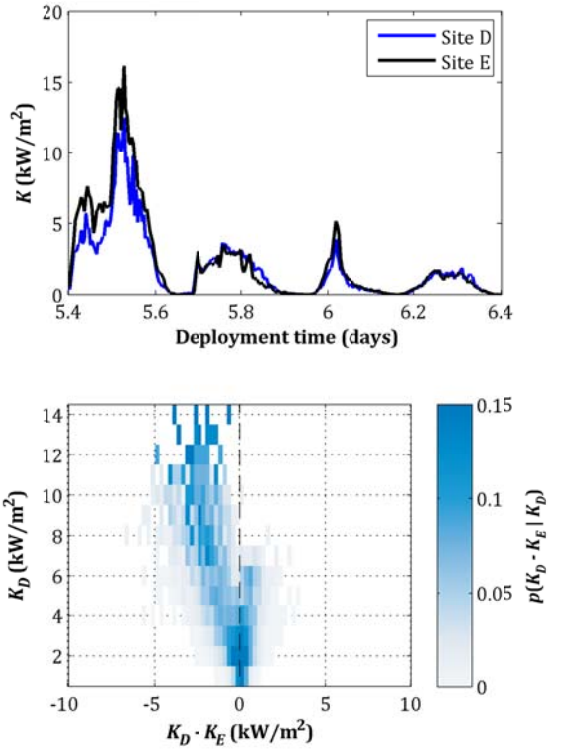

FIGURE 4. (TOP) REPRESENTATIVE TIME SERIES VARIATIONS IN POWER DENSITY BETWEEN SITES D AND E. (BOTTOM) POWER DENSITY PHASE PROBABILITY FOR SAME SITES.

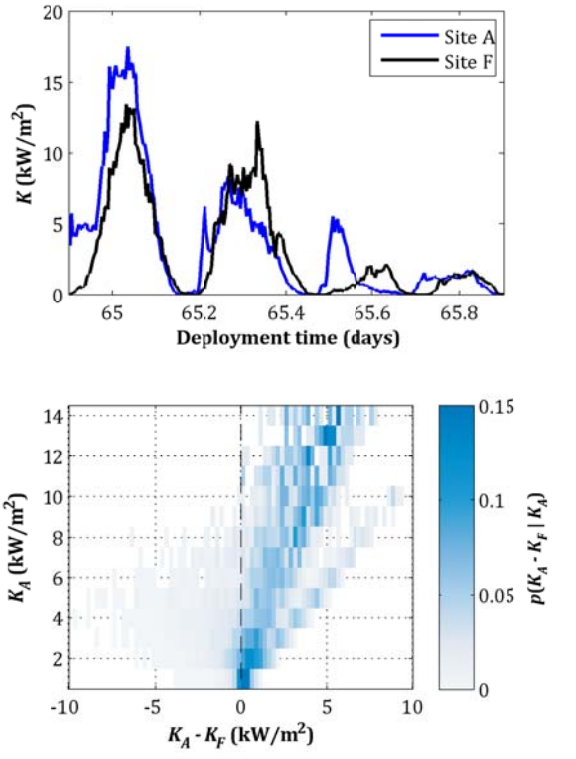

FIGURE 5. (TOP) REPRESENTATIVE TIME SERIES VARIATIONS IN POWER DENSITY BETWEEN SITES A AND F. (BOTTOM) POWER DENSITY PHASE PROABIITY FOR SAME SITES.

TABLE 3. AMPLITUDE AND PHASE OF THE PRINCIPAL SEMIDIURNAL (M2) AND DIURNAL (K1) CURRENT CONSTITUENTS (20 m ABOVE SEABED).

Pair	Site	M2		K1	
		A (m/s)	g (°)	A (m/s)	g (°)
I	A	1.63 ± 0.02	214.8 ± 0.4	0.70 ± 0.01	78.1 ± 1.2
	B	1.69 ± 0.01	214.7 ± 0.4	0.72 ± 0.01	78.3 ± 1.0
II	A	1.64 ± 0.01	214.4 ± 0.4	0.66 ± 0.01	88.7 ± 0.5
	C	1.72 ± 0.01	213.8 ± 0.5	0.69 ± 0.01	88.7 ± 0.4
III	D	1.73 ± 0.01	213.0 ± 0.4	0.50 ± 0.00	92.4 ± 0.6
	E	1.81 ± 0.01	212.3 ± 0.3	0.51 ± 0.01	93.9 ± 0.8
IV	A	1.57 ± 0.02	214.9 ± 0.6	0.51 ± 0.02	73.9 ± 1.8
	F	1.45 ± 0.01	226.3 ± 0.5	0.52 ± 0.02	77.6 ± 2.2

Collectively, these results indicate that phase variations in both the aharmonic and harmonic components of the tidal currents may contribute to co-temporal phase differences in power density. For example, the phases of the dominant harmonic constituents for Pair III are nearly identical, while substantial kinetic power phasing is shown to occur. This may suggest that the underlying mechanism for the phase difference is aharmonic, though a phase difference could also arise from the superposition of multiple minor constituents. Of course, if the dominant harmonic constituents are out of phase, then kinetic power phasing would be expected, as is the case for Pair IV (headland/center channel).

Implications of Phasing for Power Intermittency

Since the kinetic power phasing is most pronounced for pair IV (headland compared to central channel), the implications of phasing for the intermittency of power from an array was considered for these sites. A sequence of scenarios was devised in which <*P*> was held constant, but the fraction of turbines at the headland site was varied from zero to one (i.e., from all turbines in the center channel to all turbines at the headland). For scenarios involving turbines in the center channel, additional swept area is required to compensate for the lower mean power density (~20% lower in the center channel than at the headland). The result of this analysis is shown in Figure 6, with several characteristics for the hybrid arrays. The top panel shows the relative intermittency of turbine-adjusted power density

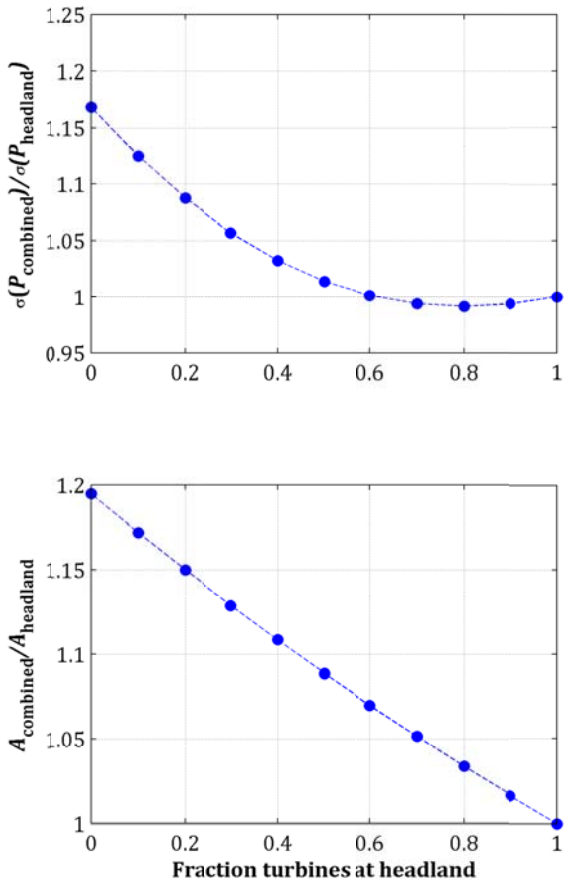

FIGURE 6. IMPLICATIONS FOR AN ARRAY DIVIDED BETWEEN THE HEADLAND (SITE A) AND CENTER CHANNEL (SITE F) LOCATIONS (CONSTANT AVERAGE ARRAY POWER OUTPUT).

intercepted by the hypothetical array. An array with 80% of its swept area near the headland has slightly lower intermittency than an array located either only at the headland or the central channel. However, this reduced intermittency comes at the cost of a 3% increase in total swept area in order to hold power output constant. This would probably not be considered economically beneficial.

We note, however, that this case represents a fairly poor scenario for the benefits of local phasing since the center channel is less energetic than the headland site and the characteristics of the tidal currents result in greater intermittency for power generation in the channel relative to the headland (for a constant rated and cut-in speed). Thyng's [6] high resolution modeling of Admiralty Inlet indicates a region of high power density adjacent to Point Wilson. Deploying turbines at both point Wilson and Admiralty Head might substantially reduce intermittency without increasing the required swept area to achieve a desired array power output.

CONCLUSIONS

Examination of temporal trends in kinetic power density between locations in a tidal channel reveals significant amplitude and phase variations. These local phase variations, observed over distances less than 5 km, suggest opportunities for smoothing array power output and reducing tidal resource intermittency. However, these benefits are only likely to be realized if locations that are out of phase have similar mean power densities. This study indicates that when evaluating the power performance of large arrays, it may not be appropriate to assume that power generation from all turbines will be in phase. These results highlight the benefit of collecting co-temporal current measurements during resource characterization activities at tidal energy sites, both to directly evaluate power phasing and to calibrate numerical models.

ACKNOWLEDGEMENTS

The authors wish to acknowledge the financial support of the US Department of Energy under DE-FG36-08GO18179. Many thanks to Joe Talbert and Alex DeKlerk for maintaining the Sea Spider platforms over several years of deployments and to Captain Andy Reay-Ellers for helping us put them in the right place.

REFERENCES

1 Polagye, B. and Thomson, J., 2013, "Tidal energy resource characterization: methodology and field study in Admiralty Inlet, Puget Sound, US," *Proc. IMechE Part A, J. Power and Energy*, doi:10.1177/0957650912470081.

2 Iyer, A.S., Couch, S.J., Harrison, G.P., and Wallace, A.R., 2013, "Variability and phasing of tidal current energy around the United Kingdom," *Renewable Energy*, **51**:343-357.

3 Mofjeld, H. and Larsen, L., 1984, "Tides and tidal currents of the inland waters of western Washington," NOAA Technical Memorandum ERL PMEL-56.

4 Thomson, J., Polagye, B., Durgesh, V., and Richmond, M.C., 2012, "Measurements of turbulence at two tidal energy sites in Puget Sound, WA," *IEEE Journal of Oceanic Engineering*, **37**: 363-374.

5 Foreman, M.G., Crawford, W.R., and Marsden, R.F., 1995, "De-tiding: theory and practice," *Quantitative Skill Assessment for Coastal Ocean Models, Coastal and Estuarine Studies*, **47**, 203-239.

6 Thyng, K.M., 2012, "Numerical simulation of Admiralty Inlet, WA, with tidal hydrokinetic turbine siting application," PhD dissertation, University of Washington, Seattle, Washington (USA).

7 Codiga, D.L., 2011, "Unified tidal analysis and prediction using the UTide matlab functions," Technical Report 2011-01, Graduate School of Oceanography, University of Rhode Island, Narragansett, RI. 59pp. ftp://www.po.gso.uri.edu/pub/downloads/codiga/pubs/2011Codiga-UTide-Report.pdf

8 Pawlowicz, R. Beardsley, and S. Lentz, 2002, "Classical tidal harmonic analysis include error estimates in MATLAB using T_TIDE", *Computers & Geosciences*, **28**(8), 929-937.

9 Kutney, T., Karsten, R., and Polagye, B., 2013, "Priorities for Reducing Tidal Energy Resource Uncertainty: Clearing the bar for Project Financing", to be presented at EWTEC 2013 in Aalborg,Denmark.